# 4 Gas and Particle Motion

PAUL A. BARON

Centers for Disease Control and Prevention, National Institute for Occupational Safety and Health, Cincinnati, OH

KLAUS WILLEKE

Department of Environmental Health, University of Cincinnati, Cincinnati, OH

## INTRODUCTION

Aerosols consist of two components: a gas or gas mixture, most commonly air; and the particles suspended in it. The behavior of the particles within the aerosol depends to a large extent on the motion and intrinsic properties of the suspending gas. Submicrometer-sized particles, especially those less than 0.1 μm diameter, are affected by the motion of individual gas molecules (the *free molecular regime*). Thus, the kinetic theory of gases is useful in understanding the behavior of these particles. Larger particles can be treated as being submersed in a continuous gaseous medium or, more broadly, a fluid (the *continuum regime*). The tools of gas or fluid dynamics are more useful for this size range. Intermediate-sized particles usually can be treated by adjustment of equations from the continuum regime. This intermediate range is termed the *transition* or *slip regime*. Whether considering a molecular ensemble or a continuous fluid, the motion of the gas will largely dictate the behavior of the suspended particles. In this chapter, concepts and parameters that affect gas and particle motion are discussed and quantified as migration and deposition parameters in specific force fields.

## BULK GAS MOTION

### Reynolds Number

When measuring an aerosol, elucidating the gas flow patterns is critical to understanding what happens to the aerosol in the environment, on its way into the sensor of the measuring instrument or in the actual sensor. While the aerosol particles follow the overall gas flow, their trajectories can deviate from the gas flow due to various external forces as well as changes in gas direction and velocity. Gas motion can be visualized by observing the streamlines, that is, tracing the motion of miniscule volumes of gas. Gas flowing around an aerosol particle can have the same flow streamline pattern as gas passing around a large object such as a basketball.

The equivalence of fluid motion for various-sized objects can be described in terms of the forces involved. The flow pattern, whether it is smooth or turbulent, is governed by the ratio

*Aerosol Measurement: Principles, Techniques, and Applications, Second Edition*, Edited by Paul A. Baron and Klaus Willeke.
ISBN 0-471-35636-0 

of the inertial force of the gas to the friction force of the gas moving over the surface. This ratio is expressed by the Reynolds number, *Re*, an extremely useful parameter when dealing with aerosols.

$$Re = \frac{\rho_g V d}{\eta} = \frac{V d}{\nu} \tag{4–1}$$

where $V$ is the velocity of the gas, $\eta$ is the dynamic gas viscosity, $\nu$ is the kinematic viscosity ($= \eta/\rho_g$), and $d$ is a characteristic dimension of the object, such as the diameter of a sphere. Because this dimensionless number characterizes the flow, it depends on gas density, $\rho_g$, not on the particle density. At normal temperature and pressure (NTP), that is, 293 K [20°C] and 101 kPa [1 atm], $\rho_g = 1.192\,\text{kg/m}^3$ [$1.192 \times 10^{-3}\,\text{g/cm}^3$] and $\eta = 1.833 \times 10^{-5}\,\text{Pa·s}$ [$1.833 \times 10^{-4}$ dyne s/cm$^2$], which reduces Eq. 4–1 to

$$\begin{aligned} \text{Re} &= 65{,}000\,Vd \quad \text{for } V \text{ in m/s and } d \text{ in m} \\ [\text{Re} &= 6.\,Vd \quad\quad \text{for } V \text{ in cm/s and } d \text{ in cm}] \end{aligned} \tag{4–2}$$

Distinction must be made between the *flow Reynolds number*, $Re_f$, and *the particle Reynolds number*, $Re_p$. Flow Reynolds number defines the gas flow in a tube or channel of cross-sectional dimension $d$. Particle Reynolds number defines the gas flow around a particle that may be found in this tube or channel flow. The characteristic dimension in the latter is particle diameter, $d_p$, and $V$ expresses the relative velocity between the particle and the gas flow. Because the difference between these velocities is generally small and the particle's dimension is very small, the particle Reynolds number usually has a very small numerical value.

### Common Gas Flows

When friction forces dominate the flow (i.e., at low Reynolds numbers), the flow is smooth, or *laminar*. Under laminar flow, no streamlines loop back on themselves. At higher Reynolds numbers, the inertial forces dominate, and loops appear in the streamlines until at still higher Reynolds numbers the flow becomes chaotic, or *turbulent*. The actual values of the Reynolds number depend on how the gas flow is bounded. For instance, laminar flow occurs in a circular duct when the flow Reynolds number is less than about 2000, while turbulent flow occurs for Reynolds numbers above 4000. In the intermediate range, the gas flow is sensitive to the previous history of the gas motion. For instance, if the gas velocity is increased into this intermediate range slowly, the flow may remain laminar. When a gas passes around a suspended object, such as a sphere, flow is laminar for particle Reynolds numbers below about 0.1.

Because often it is expensive and difficult to test collection and measurement systems at full scale and in situ, small-scale water (or other liquid) models operating at the same Reynolds number as the system being studied are a useful alternative. Dye injection into the flow stream allows visualization of the streamlines. Such models can operate on a smaller physical scale with a slower time response so that it is easy to observe the time evolution of flow patterns. The same technique can be used to model the behavior of particles.

Many gas-handling systems for instruments use cylindrical tubing to carry the aerosol from one place to the other. Understanding the flow patterns within the tubing is important for predicting the losses that occur within the tubing as well as predicting the distribution of particles within the tubing. If a gas begins to flow in a cylindrical tube, the friction at the wall slows the gas velocity relative to the motion in the center of the tube. At low Reynolds numbers, the dominating friction force produces a characteristic laminar parabolic velocity profile. The gas velocity in the center of the tube for this *Poiseuille flow* is twice that of the average velocity in the tube. Poiseuille flow does not become established immediately. A common rule of thumb is to assume that it takes 10 tube diameters for this equilibrium flow to be effectively established.

**EXAMPLE 4–1**

Silica dust of 10 μm diameter is removed by a 0.30 m diameter ventilation duct at 20 m/s (about 4000 fpm). An old rule of thumb in industrial hygiene is that silica dust of that size gravitationally settles at 1 cm/s (0.01 m/s). Calculate the flow and particle Reynolds numbers at 293 K [20°C].

*Answer*: The relevant parameters for the flow Reynolds number are the duct diameter and the gas flow velocity in the duct. From Eq. 4–2:

$$Re_f = 65{,}000\, Vd = 65{,}000\left(20\frac{\text{m}}{\text{s}}\right)0.30\text{m} = 3.90 \times 10^5$$

The relevant parameters for the particle Reynolds number are the particle diameter and the gravitational settling velocity perpendicular to the gas flow:

$$Re_p = 65{,}000\, Vd = 65{,}000\left(0.01\frac{\text{m}}{\text{s}}\right)10 \times 10^{-6}\text{m} = 6.5 \times 10^{-3}$$

The flow Reynolds number exceeds 4000, indicating turbulent flow in the ventilation duct. The particle Reynolds number is less than one, indicating that the flow around the particle can be laminar. However, it is not in this case because the gas flow is turbulent.

The region near a surface where the flow is dominated by the friction force is termed the *boundary layer*. When flow starts along a surface, in either time or space, the boundary layer consists only of the gas at the surface, where the relative velocity is zero. At low Reynolds numbers, the boundary layer grows until steady-state conditions are reached. For the cylinder flow example above, the boundary layer grows into a parabolic flow profile that fills the cylinder. At higher Reynolds numbers (in the turbulent regime) or during abrupt changes in flow conditions, the boundary layer can become separated from the surface. The development of the boundary layer and its relationship to the overall flow depends on the object immersed in the fluid. Such behavior has been described in many fluid mechanics texts (e.g., White, 1986) and especially in "Boundary-Layer Theory" (Schlichting, 1979).

There are a wide variety of flow situations for which empirical or experimentally verified theoretical solutions exist. For instance, when a gas passing through a cylindrical tube under laminar flow conditions negotiates a 90° bend, the cylindrical symmetry of the flow pattern in the tube is reduced to a plane of symmetry. Thus, the flow symmetry must also be reduced. Two circulation patterns, one sometimes described as secondary flow to differentiate it from the primary flow along the tube axis, are set up on either side of the plane of the bend, as shown in Figure 4–1. This secondary flow causes mixing of the gas as well as increased inertial forces on particles suspended in the gas (Tsai and Pui, 1990). In tubing used to transport aerosols, bends are generally undesirable because of increased particle loss.

For various reasons, there are often constrictions or expansions in a tube carrying a gas. A constriction will force the gas to increase in velocity and be focused in the center of the tubing, even more than the constriction in size. After this contraction region, or *vena contracta*, the gas flow eventually expands again to fill the tubing and re-establishes an equilibrium pattern. These disturbances will also cause increased particle deposition.

When a gas flows from an initial tube diameter into a suddenly expanded section or into free space, the flow pattern may persist for many initial tube diameters downstream. If the expansion of the tube is very slight, the flow does not separate from the walls, and the flow pattern can expand smoothly to fill the increased diameter of the tube. In general, the angle

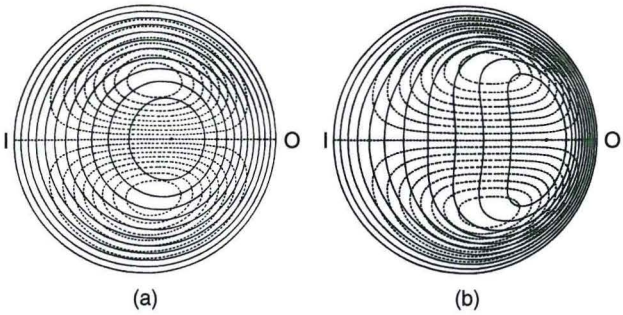


**Fig. 4–1.** Secondary flow streamlines (dotted lines) and primary flow velocity contours (solid lines) at a short distance downstream from the exit plane of a 90° bend in a tube. I and O refer to the inner and outer sides of the bend, respectively. The flows are calculated at two Dean numbers:

$$De = Re/\sqrt{\text{bend radius/tube radius}}$$

**a**, $De = 17$. **b**, $De = 107$. (From McConalogue and Srivastaval, 1968, with permission of the Royal Society.)

between the wall and the tube axis needs to be less than 7° to avoid flow separation from the tube wall.

### Gas Density and Mach Number

The density of a gas, $\rho_g$, is related to its temperature, $T$, and pressure, $P$, through the *equation of state*:

$$P = \rho_g \frac{R_u}{M} T = \rho_g R T \tag{4–3}$$

where $\rho_g$ is the gas density (1.192 kg/m$^3$ [$1.192 \times 10^{-3}$ g/cm$^3$] for air at NTP), $T$ is the absolute gas temperature in K, $M$ is the molecular weight in kg/mol, and $R_u$ is the universal gas constant (= 8.31 Pa·m$^3$/mol·K [$8.31 \times 10^7$ dyne·cm/mol·K]). In air, the effective molecular weight is 0.0289 kg/mol [28.9 g/mol]. Thus, the specific gas constant for air is $R$ = 288 Pa·m$^3$/kg·K [$2.88 \times 10^6$ dyne·cm/g·K]. One atmosphere equals 101 kPa, where 1 Pa = 1 N/m$^2$ = 10 dyne/cm$^2$.

When this gas moves at a high velocity relative to the acoustic velocity, $U_g$, in that gas, the gas becomes compressed. The degree of compression depends on the *Mach number*, *Ma*:

$$Ma = \frac{U}{U_{\text{sonic}}} \tag{4–4}$$

Here, the gas velocity is designated as $U$ to distinguish it from particle velocity $V$. When $Ma << 1$, the gas flow is considered incompressible. This is true in most aerosol sampling situations. In air, the sonic or sound velocity at ambient temperature is about 340 m/s (1100 ft/s).

## TRANSITION AND GAS MOLECULAR FLOW

### Knudsen Number

Large aerosol particles are constantly bombarded from all directions by a great number of gas molecules. When a particle is small, less than 1 μm in size, its location in space may be affected by bombardment of individual gas molecules. Its motion is then no longer determined by continuum flow considerations, but by gas kinetics.

**TABLE 4–1. Gas Properties for Several Gases at NTP (293.15 K and 101.3 kPa)**

| Gas | $\eta$ ($10^{-6}$ Pa·s) | $S$ (K) | $\rho_g$ (kg/m$^3$) | $\lambda$ (μm) |
|---|---|---|---|---|
| Air | 18.203 | 110.4 | 1.205 | 0.0665 |
| Ar | 22.292 | 141.4 | 1.662 | 0.0694 |
| He | 19.571 | 73.8 | 0.167 | 0.192 |
| $H_2$ | 8.799 | 66.7 | 0.835 | 0.123 |
| $CH_4$ | 10.977 | 173.7 | 0.668 | 0.0537 |
| $C_2H_6$ | 9.249 | 223.2 | 1.264 | 0.0328 |
| $i$-$C_4H_{10}$ | 7.433 | 255.0 | 2.431 | 0.0190 |
| $N_2O$ | 14.646 | 241.0 | 1.837 | 0.0433 |
| $CO_2$ | 14.673 | 220.5 | 1.842 | 0.0432 |

*Source*: Adapted from Rader (1990).

The *average velocity of a molecule*, $\overline{V}$, is a function of its molecular weight, $M$, and the gas temperature, $T$. In air ($M_{air} = 0.0289$ kg/mol) at normal temperature and pressure (NTP, 20°C, 1 atm), this molecular velocity is 463 m/s. Using these air reference values, the average velocity can be estimated for other gases and temperatures:

$$\overline{V} = \overline{V}_r \left(\frac{T}{T_r}\right)^{1/2} \left(\frac{M_r}{M}\right)^{1/2} \tag{4–5}$$

*Mean free path*, $\lambda$, is the mean distance a molecule travels before colliding with another molecule. In air at 293 K and atmospheric pressure, the mean free path, $\lambda_r$, is 0.0664 μm. The mean free path is an abstraction that is determined from a kinetic theory model that relates it to the coefficient of viscosity. Using these reference values, $\lambda$ is determined for other pressures and temperatures (Willeke, 1976):

$$\lambda = \lambda_r \left(\frac{101}{P}\right)\left(\frac{T}{293}\right)\left(\frac{1+110/293}{1+110/T}\right) \tag{4–6}$$

where $P$ is in kPa and $T$ in K. If the unit of atmosphere is used for pressure, the factor of 101 used in Eq. 4–6 is substituted by one. The factor of 110 (K) is the Sutherland constant, and the value changes for different gases. The mean free path and the average molecular velocity are parameters that are frequently used to predict bulk properties of a gas, such as thermal conductivity, diffusion, and viscosity. Mean free paths for other gases are presented in Table 4–1.

The *Knudsen number*, $Kn$, relates the gas molecular mean free path to the physical dimension of the particle, usually the *particle radius*, $r$.

$$Kn = \frac{\lambda}{r} = \frac{2\lambda}{d_p} \tag{4–7}$$

where $d_p$ is the physical diameter of the particle. The Knudsen number is somewhat counterintuitive as an indicator of particle size because it has an inverse size dependence. $Kn << 1$ indicates continuum flow, and $Kn >> 1$ indicates free molecular flow. The intermediate range, approximately $Kn = 0.4$ to 20, is usually referred to as the transition or slip flow regime.

### Slip Flow Regime and Correction Factor

If a particle is much smaller than the gas molecular mean free path ($Kn >> 1$), it can travel past an obstacle at a very small distance from the object because no gas molecule may impede

it. If the particle is very large ($Kn << 1$), many gas molecular collisions occur near the surface and the particle is decelerated. When the Knudsen number is the order of unity, the particle may slip by the obstacle. When the particle size is in this *slip flow regime*, it is convenient to assume that the particle is still moving in a continuum gas flow. To accommodate for the difference, a slip correction factor, $C_c$, also referred to as the *Cunningham slip correction factor*, is introduced into the equations. An empirical fit to air data for particles gives (Allen and Raabe, 1985)

$$C_c = 1 + Kn[\alpha + \beta \exp(-\gamma / Kn)] \tag{4–8}$$

Various values for $\alpha$, $\beta$, and $\gamma$ have been reported. However, it is important to use the mean free path with which these constants were determined. The value of $\lambda_r$ used in Eq. 4–6 should also be consistent with the derivation of the slip coefficient constants. The following constants are consistent with $\lambda_r = 0.0664\,\mu m$ at NTP. For solid particles, $\alpha = 1.142$; $\beta = 0.558$; $\gamma = 0.999$ (Allen and Raabe, 1985). For oil droplets, $\alpha = 1.207$; $\beta = 0.440$; $\gamma = 0.596$ (Rader, 1990). $C_c$ for other gases such as $CO_2$ and He are similar within a few percent. The slip correction and viscosity values are better determined than most other aerosol-related parameters and are therefore reported with a higher degree of precision.

For pressures other than atmospheric, the slip correction changes because of the pressure dependence of the mean free path in $Kn$, and the following may be used for solid particles:

$$C_c = 1 + \frac{1}{Pd_p}[15.60 + 7.00 \exp(-0.059 Pd_p)] \tag{4–9}$$

where $P$ is the absolute pressure in kPa, and $d_p$ is the particle diameter in μm (Hinds, 1999).

$C_c$ is one in the continuum regime and becomes greater than one for decreasing particle diameter in the transition regime. For instance, $C_c = 1.02$ for 10 μm particles; 1.15 for 1 μm particles, and 2.9 for 0.1 μm particles. Note that the shape factor and the slip correction must be consistent with the type of equivalent diameter used in the same equation (Brockmann and Rader, 1990). For further discussion of shape factor, see Chapter 23.

### Gas Viscosity

*Gas viscosity* is primarily due to the momentum transfer that occurs during molecular collisions. These frequent and rapid collisions tend to damp out differences in bulk gas motion as well as impede the net motion of particles relative to the gas. Thus, the mobility of a particle in a force field depends on the aerodynamic drag exerted on the particle through the gas viscosity. Fluid dynamic similitude, as expressed by Reynolds number, depends on gas viscosity, $\eta$. Therefore, knowledge of the gas viscosity is important when dealing with aerosol particle mechanics. The viscosity can be related to a reference viscosity $\eta_r$ and a reference temperature, $T_r$, as follows:

$$\eta = \eta_r \left( \frac{T_r + S}{T + S} \right) \left( \frac{T}{T_r} \right)^{3/2} \tag{4–10}$$

where $S$ is the Sutherland interpolation constant (Schlichting, 1979). Note that viscosity is independent of pressure.

In SI units, viscosity is expressed in Pa·s. In cgs units, viscosity is expressed in dyne s/cm$^2$, also referred to as *poise* or *P*. For air at 293 K, the viscosity is $1.833 \times 10^{-5}$ Pa·s [183.3 μpoise] and S = 110.4 K. The interpolation formula is fitted to the data over the range 180 to 2000 K (Schlichting, 1979). Reference values of viscosity and Sutherland constants for other gases are presented in Table 4–1.

## GAS AND PARTICLE DIFFUSION

The random movement of the gas molecules causes gas and particle diffusion if there is a concentration gradient. For instance, in a diffusion denuder, $SO_2$ gas molecules may diffuse to an absorbing surface due to their high diffusivity. Sulfate particles, which are larger and therefore have lower diffusivity, will mostly be transported through the device. Thus, the $SO_2$ gas molecules are separated from the sulfate particles.

### Gas Diffusion

Diffusion always causes net movement from a higher concentration to a lower one. The *net flux* of gas molecules, $J$, is in the direction of lower concentration. Thus, in simple one-dimensional diffusion,

$$J = -D\frac{\partial N}{\partial x} \tag{4–11}$$

where $x$ is the direction of diffusion, $N$ is the concentration, and $D$ is a proportionality constant referred to as the *diffusion coefficient*. The diffusion coefficient for a gas with molecular weight, $M$, is (Hinds, 1999:27)

$$D = \left(\frac{3\sqrt{2}\pi}{64Nd_{\text{molec}}^2}\right)\left(\frac{RT}{M}\right)^{1/2} \tag{4–12}$$

where $N$ is the number of gas molecules/m$^3$ and $d_{\text{molec}}$ is the molecular collision diameter ($3.7 \times 10^{-10}$ m for air). The diffusion coefficient of air molecules at 293 K is $1.8 \times 10^{-5}$ m$^2$/s. This predicts a diffusion coefficient that is approximately 10% below the correct value (Hinds, 1999:27).

### Particle Diffusion

Small particles can achieve significant diffusive motion in much the same fashion as des-cribed for gas molecules. The difference is only in the particle size and shape. Because of their increase in inertia with particle mass and the larger surface area over which the bombardment by the gas molecules is averaged, large particles will diffuse more slowly than small particles. For particles in a gas, the *diffusion coefficient* or *diffusivity*, $D$, can be computed by

$$D = \frac{kTC}{3\pi\eta d_p} = kTB \tag{4–13}$$

where $k$, the Boltzmann constant, is $1.38 \times 10^{-23}$ N·m/K [$1.38 \times 10^{-16}$ dyne·cm/K] and the mechanical mobility, $B$ in m/N·s [cm/dyne·s], is a convenient aerosol property that combines particle size with some of the properties of the suspending gas

$$B = \frac{C_c}{3\pi\eta d_p} \tag{4–14}$$

Particle diffusion, also referred to as *Brownian motion*, occurs because of the relatively high velocity of small particles, and it is sometimes useful to estimate how far, on the average, these particles move in a given time. The *root mean square* (rms) *distance*, $x_{\text{rms}}$, that the particles can travel in time, $t$, is

$$x_{\text{rms}} = \sqrt{2Dt} \tag{4–15}$$

**EXAMPLE 4–2**

Fume aerosols of 0.01 μm diameter are drawn into the deep lung regions of a worker whose alveoli can be approximated by 0.2 mm diameter spheres. We would like to estimate if these particles are likely to deposit in this area of the lungs during a breath-holding period of 4 seconds. Assume that body temperature is 330 K [37°C].

*Answer*: We note that calculation of $x_{rms}$ (Eq. 4–15) requires knowledge of the diffusion coefficient, which in turn requires the slip correction factor and viscosity. To simplify the calculation, let us assume for the moment that the diffusion is taking place at room temperature. Thus, the air viscosity is $1.83 \times 10^{-5}$ Pa·s and the mean free path is 0.0665 μm. (For a more exact estimate of these parameters at body temperature, use Eqs. 4–6 and 4–10, respectively.)

The slip correction factor can be determined from Eq. 3–8 using constants for solid particles:

$$C_c = 1 + Kn[1.142 + 0.558\exp(-0.999/Kn)]$$

$$C_c = 1 + \frac{2 \cdot 0.0665\,\mu\text{m}}{0.01\,\mu\text{m}}\left[1.142 + 0.558\exp\left(-0.999\frac{0.01\,\mu\text{m}}{2 \cdot 0.0665\,\mu\text{m}}\right)\right] = 23.1$$

We then estimate the diffusion coefficient, using Eq. 3–13:

$$D = \frac{kTC_c}{3\pi\eta d_p}$$

$$D = \frac{\left(1.38 \times 10^{-23}\,\frac{N \cdot m}{K}\right)(293\text{ K})(23.1)}{3 \cdot 3.14 \cdot (1.83 \times 10^{-5}\,\text{Pa·s})\left(0.01\,\mu\text{m} \times 10^{-6}\,\frac{\text{m}}{\mu\text{m}}\right)} = 5.42 \times 10^{-8}\,\frac{\text{m}^2}{\text{s}}$$

$$\left[D = \frac{\left(1.38 \times 10^{-16}\,\frac{\text{dyn·cm}}{\text{K}}\right)(293\text{ K})(23.1)}{3 \cdot 3.14 \cdot (1.83 \times 10^{-4}\,\text{poise})\left(0.01\mu\text{m} \times 10^{-4}\,\frac{\text{cm}}{\mu\text{m}}\right)} = 5.42 \times 10^{-4}\,\frac{\text{cm}^2}{\text{s}}\right]$$

Finally, using Eq. 3–15:

$$x_{rms} = \sqrt{2Dt} = \sqrt{2\left(5.42 \times 10^{-8}\,\frac{\text{m}^2}{\text{s}}\right)(4\text{ s})}$$

$$= 6.60 \times 10^{-4}\text{m}[0.0660\text{ cm}] = 0.660\text{ mm}$$

We find that, at room temperature, the rms displacement by diffusion is much larger than the alveolar size. At the elevated temperature in the lung (37°C), the particles are expected to move faster and diffuse further. If this air termperature is used in the calculation of the diffusion coefficient, $x_{rms}$ is 0.675 mm. Thus, we know that most of these particles are likely to be collected in the alveolar space of the lung. A more exact analysis can be made by considering such factors as the spherical geometry of the alveoli, the location of the particles within the alveoli, and the air temperature.

By including the air temperature dependence also in the calculation of viscosity and mean free path, the rms displacement calculation results in 0.661 mm.

**TABLE 4–2. Particle Parameters for Unit Density Particles at NTP**

| Particle Diameter, $d_p$ (μm) | Slip Correction Factor, $C_c$ | Settling Velocity, $V_{grav}$ (m/s) | Relaxation Time, $t$ (s) | Stopping Distance, $S$ $V_0 = 10$ m/s (m) | Mobility, $B$ (m/N·s) | Diffusion Coefficient, $D$ (m²/s) | rms Brownian Displacement in 10 s (m) |
|---|---|---|---|---|---|---|---|
| 0.00037[a] | | | $2.6 \times 10^{-10}$ | $2.5 \times 10^{-9}$ | $9.7 \times 10^{15}$ | $1.8 \times 10^{-5}$[b] | $2.8 \times 10^{-2}$ |
| 0.01 | 23.04 | $6.95 \times 10^{-8}$ | $7.1 \times 10^{-9}$ | $7.1 \times 10^{-8}$ | $1.4 \times 10^{13}$ | $5.5 \times 10^{-8}$ | $1.0 \times 10^{-3}$ |
| 0.1 | 2.866 | $8.65 \times 10^{-7}$ | $8.8 \times 10^{-8}$ | $8.8 \times 10^{-7}$ | $1.7 \times 10^{11}$ | $6.8 \times 10^{-10}$ | $1.2 \times 10^{-4}$ |
| 1 | 1.152 | $3.48 \times 10^{-5}$ | $3.5 \times 10^{-6}$ | $3.5 \times 10^{-5}$ | $6.8 \times 10^{9}$ | $2.7 \times 10^{-11}$ | $2.3 \times 10^{-5}$ |
| 10 | 1.015 | $3.06 \times 10^{-3}$ | $2.3 \times 10^{-4}$ | $2.3 \times 10^{-3}$ | $6.0 \times 10^{8}$ | $2.4 \times 10^{-12}$ | $7.0 \times 10^{-6}$ |
| 100 | 1.002 | $2.61 \times 10^{-1}$ | $1.3 \times 10^{-2}$ | 0.13 | $5.9 \times 10^{7}$ | $2.4 \times 10^{-13}$ | $2.2 \times 10^{-6}$ |

[a] Average diameter of a molecule in air.
[b] Calculated using Eq. 3–12.

Table 4–2 includes examples of $x_{rms}$ for various-sized particles after a period of 10 s.

### Peclet Number

The amount of convective transport of particles toward an object may be related to the diffusive transport through the dimensionless *Peclet number*, *Pe*,

$$Pe = \frac{Ud_c}{D} \tag{4–16}$$

where $d_c$ is the significant dimension of the particle collecting surface and $U$ is the upstream gas velocity toward the surface. The larger the value of *Pe*, the less important is the diffusional process (Licht, 1988:226). *Pe* is often used in the description of diffusional deposition on filters. For further discussions of diffusions, see Chapters 8, 9, and 19.

### Schmidt Number

The ratio of the Peclet number, Eq. 4–16, to the Reynolds number, Eq. 4–1, is referred to as the *Schmidt number*, *Sc*. It expresses the ratio of kinematic viscosity to diffusion coefficient.

$$Sc = \frac{\eta_g}{\rho_g D} = \frac{\nu}{D} \tag{4–17}$$

As the Schmidt number increases, convective mass transfer increases relative to Brownian diffusion of particles. It has been used for describing diffusive transport in flowing fluids (convective diffusion), especially in the development of filtration theory (Friedlander, 1977). *Sc* is relatively independent of temperature and pressure near standard conditions.

## AERODYNAMIC DRAG ON PARTICLES

Externally applied forces on an aerosol particle are opposed and rapidly balanced by the aerodynamic drag force. An example of this is a sky diver: The gravitational force pulling the sky diver toward the earth is eventually balanced by the air resistance, and the diver reaches a final falling speed of about 63 m/s (140 miles per hour).

A particle's drag force, $F_{drag}$, relates the resistive pressure of the gas to the velocity pressure given by the relative motion between the particle and the surrounding gas. When the particle dimensions are much larger than the distance between the gas molecules, the

surrounding gas can be considered a continuous fluid (continuum regime). Under this condition, the *drag force* is given by

$$F_{drag} = \frac{\pi}{8} C_d \rho_g V^2 d_p^2 \tag{4–18}$$

Note that the aerodynamic drag is related to the gas density, $\rho_g$, not the particle density. The *drag coefficient*, $C_d$, relates the drag force to the velocity pressure. When the inertial force pushing the gas aside, due to the velocity difference between the gas and the particle, is much smaller than the viscous resistance force, the drag coefficient, $C_d$, is expressed in terms of gas flow parameters

$$C_d = \frac{24}{Re_p} \qquad Re_p < 0.1 \tag{4–19}$$

where $Re_p$ is the particle Reynolds number. This relationship is accurate within 1% in the $Re_p$ range indicated. If 10% accuracy is acceptable, Eq. 4–19 can be used up to $Re_p < 1.0$. Combining Eqs. 4–1, 4–18, and 4–19 results in

$$F_{drag} = 3\pi\eta V d_p \tag{4–20}$$

This equation is also known as *Stokes' law*. For Stokes' law flow of gas around the particle, the drag on the particle depends only on gas viscosity, $\eta$, particle velocity, $V$, and particle diameter, $d_p$. This assumes that the particle is spherical. The particle drag for shapes other than spheres is usually difficult to predict theoretically. Therefore, for particles of other shapes, a *dynamic shape factor* $\chi$ is introduced that relates the motion of the particle under consideration to that of a spherical particle

$$F_{drag} = 3\pi\eta V \chi d_m \tag{4–21}$$

where $d_m$ is now the *mass equivalent diameter* defined as the diameter of a sphere composed of the particle bulk material with no voids that has the same mass as the particle in question. The shape factor is sometimes related to the equivalent volume or *volume equivalent diameter*, $d_{ev}$, defined as the diameter of a sphere of equivalent volume. This term may be ambiguous. When the equivalent volume is composed of particle bulk material with no void, $d_{ev} = d_m$. However, if the material includes voids, $d_{ev} > d_m$. If we determine the shape factors and equivalent diameters for particles that we wish to measure, the behavior of the particles can be predicted when they are influenced by various force fields (e.g., gravity or electrostatic).

We know that gases are not continuous fluids, as indicated above, but consist of discrete molecules. Therefore, when the particle size approaches the mean free path of the gas molecular motion (transition or slip regime), we can apply a correction that takes the "slip" between the particle and the gas into account. Thus, the Cunningham slip correction factor $C_c$ is introduced into Eq. 4–21:

$$F_{drag} = \frac{3\pi\eta V \chi d_{ev}}{C_c} \tag{4–22}$$

Eq. 4–22 assumes that the flow around the particle is laminar. As particles move faster (i.e., have a larger $Re_p$), the above relationships must be modified further. As indicated above, the range over which Eq. 4–19 is accurate defines the Stokes regime. For larger $Re_p$, empirical relationships for $C_d$ have been developed to extend Stokes' law. The drag coefficient, $C_d$, for a spherical particle is the ratio of the resistance pressure due to aerodynamic drag (drag force/cross-sectional area) to the velocity pressure of the flow toward the sphere based on the relative velocity between the particle and the suspending gas. Figure 4–2 shows the relationship of the drag coefficient to particle Reynolds number over a wide range of Reynolds numbers.

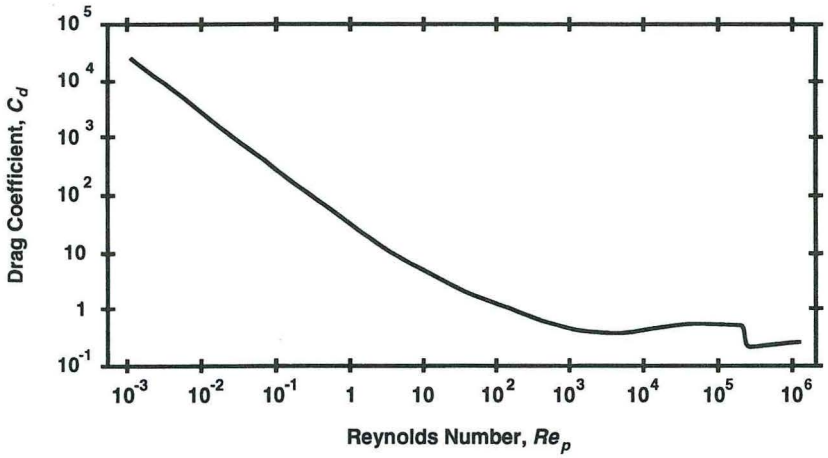


**Fig. 4–2.** Drag coefficient as a function of particle Reynolds number for spherical particles.

For $Re_p$ above 0.1, Sartor and Abbott (1975) developed the following empirical relationship:

$$C_d = \frac{24}{Re_p}(1 + 0.0196 Re_p) \qquad 0.1 \le Re_p < 5 \tag{4–23}$$

Serafini (Friedlander, 1977:105) developed the following:

$$C_d = \frac{24}{Re_p}(1 + 0.158 Re_p^{2/3}) \qquad 5 \le Re_p < 1000 \tag{4–24}$$

Note that these relationships have been derived from data obtained with smooth spheres. Similar relationships have been derived and reviewed for particles such as droplets, solid spheroids, disks, and cylinders (Clift et al., 1978:142). Typically, $Re_p$ is based on the equatorial diameter for disks and spheroids and on the cylinder diameter for cylinders, although other definitions can be used. Particles with extreme shapes may have a significantly different drag coefficient. For instance, $C_d$ for fibers is up to four times lower than for spheres with $Re_p < 100$ when the fiber diameter is used as the significant dimension in the Reynolds number expression, Eq. 4–1.

Thus, by using the appropriate form of the drag coefficient (Eq. 4–19, 4–23, or 4–24) and including the shape factor and slip coefficient, the drag force can be calculated over a wide range of particles and conditions:

$$F_{drag} = \frac{\pi C_d \rho_g V^2 \chi^2 d_{ev}^2}{8 C_c} \tag{4–25}$$

For further discussion of shape factors and behavior of nonspherical particles, see Chapter 23.

## PARTICLE MOTION DUE TO GRAVITY

The *gravitational force*, $F_{grav}$, is proportional to particle mass, $m_p$, and gravitational acceleration, $g$,

$$F_{grav} = m_p g = (\rho_p - \rho_g) v_p g \approx \rho_p v_p g \tag{4–26}$$

where $\rho_g$ is the gas density. The gravitational pull depends on the difference between the density of the particle and that of the surrounding medium. For a particle in water, this buoyancy effect is significant. For a particle in air, the buoyancy effect can be neglected for compact

particles because the particle density is generally much greater than the density of the gas. If the particle is spherical, particle volume $v_p$ can be replaced with $\pi d_p^3/6$:

$$F_{grav} = \frac{\pi}{6} d_p^3 \rho_g g \tag{4–27}$$

The gravitational field of the earth was mentioned in the previous chapter. This field exerts a force pulling a particle down. As the particle begins to move, the gas surrounding the particle exerts an opposing drag force, which, after a short period of acceleration, equals the gravitational force, and the particle reaches its terminal settling velocity. By equating the drag force, Eq. 4–18 (with Cunningham slip correction factor $C_c$ added), to the gravitational force, Eq. 4–27, and using Eq. 4–19 for $C_d$ and Eq. 4–1 for $Re_p$, the following relationship is obtained for the spherical particle settling velocity, $V_{grav}$, in the Stokes regime (Eq. 4–19):

$$V_{grav} = V_{ts} = \frac{\rho_p d_p^2 g C_c}{18\eta} \qquad Re_p < 0.1 \tag{4–28}$$

To reflect the equilibrium between the two opposing forces, this velocity is also referred to as *terminal settling velocity*, $V_{ts}$. For spherical particles with negligible slip ($C_c = 1$) and $1 < d_p < 100$, this equation reduces to the following at NTP:

$$V_{grav} \cong 3 \times 10^{-8} \rho_p d_p^2$$
$$[V_{grav} \cong 0.003 \rho_p d_p^2] \text{ in cgs units} \tag{4–29}$$

where $\rho_p$ is in kg/m$^3$ [g/cm$^3$] and $d_p$ is in μm. Spherical particles (e.g., droplets), are common in nature, and their motion can be described mathematically. Therefore, behavior of non-spherical particles is often referenced to such particles through comparison of their behavior in a gravitational field.

**EXAMPLE 4–3**

An open-faced filter cassette samples at 2 L/min ($3.33 \times 10^{-5}$ m$^3$/s [33.3 cm$^3$/s]) over its inlet face of about 35 mm diameter. If the cassette is held facing downward, can a 25 μm diameter particle with a density of 3000 kg/m$^3$ [3 g/cm$^3$ ] be drawn upward onto the filter in calm air?

*Answer*: The cassette samples at a flow rate $Q$ over a cross-sectional filter area $A$. The upward air velocity, $U$, is

$$U = \frac{Q}{A} = \frac{3.33 \times 10^{-5} \frac{\text{m}^3}{\text{s}}}{\pi \left( \frac{0.035 \text{ m}}{2} \right)^2} = 0.0346 \text{ m/s} [3.46 \text{ cm/s}]$$

The gravitational settling velocity of the 25 μm particle is, from Eq. 4–29,

$$V_{grav} = 3 \times 10^{-8} \rho_p d_p^2 = 3 \times 10^{-8} \left( 3000 \frac{\text{kg}}{\text{m}^3} \right) \left( 25 \text{ μm} \cdot 10^{-6} \frac{\text{m}}{\text{μm}} \right)$$

$$\left[ V_{grav} = 0.003 \rho_p d_p^2 = 0.003 \left( 3 \frac{\text{g}}{\text{cm}^3} \right) (0.0025 \text{ cm})^2 \right]$$
$$= 0.0563 \text{ m/s} [5.63 \text{ cm/s}] > 0.0346 \text{ m/s} [3.46 \text{ cm/s}]$$

The particle cannot be drawn upward into the sampler.

This is also the principle of a vertical elutriator, which prevents particles above a certain size from passing through the device. However, in some implementations of this device (e.g., the cotton dust elutriator) inlet effects complicate the penetration efficiency.

The *aerodynamic diameter*, $d_a$, of a particle is the diameter of a standard-density sphere that has the same settling velocity as the particle in question, as shown in Eqs. 3–1 to 3–3. Another definition that is also commonly used is the *Stokes diameter*, $d_s$, which is the diameter of a spherical particle with the same density and settling velocity as the particle in question. The aerodynamic diameter can be related to the Stokes diameter through the settling velocity equation:

$$\rho_p d_s^2 = \rho_0 d_a^2 \tag{4–30}$$

A number of instruments, including the horizontal and the vertical elutriators (see Chapters 8, 10, 25, 26), use settling velocity to separate particles according to size. For instance, aerosol particles of a certain size, $d_p$, initially spread throughout a quiescent rectangular chamber or room of height $H$, will settle at a constant velocity, $V_{grav}$. After some time, $t$, the particle concentration in the chamber, $N(t)$, will be

$$N(t) = N_0\left(1 - \frac{V_{grav}t}{H}\right) \tag{4–31}$$

where $N_0$ is the initial particle concentration in the chamber. After time $t$, a vertical distance of $V_{grav} \cdot t$ is cleared of particles. The same relationship determines the concentration of particles in a rectangular channel with air flowing through it (a horizontal elutriator). At some distance downstream of the entrance to the channel (where the aerosol concentration is $N_0$), the concentration will be $N(t)$, where $t$ is the time needed to reach that distance.

The above discussion of particle settling describes the behavior of particles in still air, a condition that is not often achieved in the environment or even in the laboratory. When the gas in a container undergoes continual and random motion, such as in a room with several randomly directed fans, the particles undergo *stirred settling*. The time-dependent concentration, $N(t)$, under these conditions is also expressed in terms of an initial particle concentration, $N_0$, the gravitational settling velocity in still air, $V_{grav}$, and the height of the container, $H$:

$$N(t) = N_0 \exp\left(\frac{-V_{grav}t}{H}\right) \tag{4–32}$$

This equation applies to any container shape with vertical walls and a horizontal bottom. This indicates that even under stirred or turbulent conditions, larger particles (higher settling velocities) will settle out more rapidly than smaller particles, even though some of the large particles may persist in the air for a long time because of the exponential decay. Note that the forms of Eqs. 4–31 and 4–32 are similar except for the exponential decay when stirring takes place during the settling. This similarity in form occurs for all such comparisons of uniform and stirred settling.

### Gravitational Settling at Higher Reynolds Numbers

Particle settling velocity can be calculated accurately for $Re_p < 0.1$ using Eq. 4–28. At higher Reynolds numbers, the observed settling velocity is lower than predicted by that equation because the drag coefficient is higher than predicted by Eq. 4–19. For spherical particles ($c = 1$), the gravitational settling velocity can be expressed as a function of $C_d$ by equating the drag force, Eq. 4–25, to the gravitational force Eq. 4–27:

$$V_{grav} = \left(\frac{4\rho_p C_c d_p g}{3\rho_g C_d}\right)^{1/2} \tag{4–33}$$

The drag coefficient has a complex dependence on the settling velocity, and Eq. 4–33 therefore cannot be solved in closed form. Graphical (Licht, 1988:160) and tabular (Hinds, 1999:56) determinations of the settling velocity at high Reynolds numbers have been used. Using Eq.

4–33 and the drag coefficient equation for the appropriate Reynolds number (e.g., Eq. 4–23 or 4–24), an iterative solution for the settling velocity can readily be obtained with a computer or calculator. A guess for $C_d$ allows the calculation of an initial value for $V_{grav}$, which is then used to calculate a new value of $C_d$. The new value of $C_d$ is then used in Eq. 4–33, and the iteration is continued until the values converge.

## PARTICLE PARAMETERS

The gravitational force effectively removes large particles from the suspending gas. Particles of 1 μm or smaller take a long time to settle (see Table 4–2, below). To settle these, the removal force is increased by, for example, rotating the gas volume, as in a centrifuge. Other devices channel the gas flow in a circular fashion (e.g., cyclones) or through bends (e.g., impactors) to create an increased force field. The following parameters are useful for describing the inertial and settling behavior of particles.

### Relaxation Time and Stopping Distance

With the Stokes settling velocity relationship (Eq. 4–28), several useful particle parameters can be defined. The first is the *particle relaxation time*:

$$\tau = \frac{\rho_p d_p^2 C_c}{18\eta} \tag{4–34}$$

This is the time a particle takes to reach 1/e of its final velocity when subjected to a gravitational field. The relaxation period is typically quite short, as indicated in Table 4–2, and can therefore be neglected for most practical applications. Use of this parameter simplifies the expression for *gravitational settling velocity* to

$$v_{grav} = \tau g \tag{4–35}$$

**EXAMPLE 4–4**

A grinding wheel dislodges many wheel and workpiece particles and projects them from the contact point toward the receiving hood of the ventilation system. A particle of a certain size and density is projected 10 mm away. How far will a particle twice this size be projected? Estimate the projected distance when the speed of the grinding wheel is doubled.

*Answer*: The projected distance is proportional to the stopping distance. From Eqs. 4–34 and 4–36,

$$S = V_0 \tau \propto V_0 \rho_p d_p^2$$

The stopping distance depends on the square of the particle diameter, so a two times larger particle will project four times the distance to 40 mm. At twice the grinding wheel speed, the particle will come off at approximately twice the initial velocity, resulting in a doubling of the distance to 20 mm.

The above stopping distance equation assumes that the particle is in the Stokes regime. If the particle diameter and velocity are such that $Re_p$ is larger than 0.1, the stopping distance will be somewhat less than quadrupled for the larger particle. This is because the drag increases faster with diameter outside the Stokes regime (see Fig. 4–2). Similarly, increasing the initial velocity also increases $Re_p$ and results in somewhat less than doubling of the distance.

Quite often, a particle, rather than starting from rest in a gravitational field, is injected into the air with an initial velocity, $V_0$. For instance, such a particle might be released from a rotating grinding wheel. The product of the relaxation time and the initial particle velocity is referred to as the *stopping distance*, $S$:

$$S = V_0 \tau \tag{4–36}$$

where $S$ is in m. Values of $S$ for an initial velocity of 10 m/s are given in Table 4–2. The concept of stopping distance is useful, for example, in impactors when evaluating how far a particle moves across the air streamlines when the flow makes a right angle bend.

Because Eq. 4–28 is accurate only in the Stokes regime, the following empirical relationship can be used at higher $Re_p$ (Mercer, 1973:41):

$$S = \frac{\rho_p d_p}{\rho_g}\left(Re_0^{1/3} - \sqrt{6}\arctan\left(\frac{Re_0^{2/3}}{\sqrt{6}}\right)\right) \qquad 1 < Re_p < 400 \tag{4–37}$$

where $Re_0$ is the Reynolds number of the particle at the initial velocity.

### Stokes Number

When gas flow conditions change suddenly, as at the particle collection surface of an impactor, the ratio of the stopping distance to a characteristic dimension, $d$, is defined as the *Stokes number*, *Stk*:

$$Stk = \frac{S}{d} \tag{4–38}$$

The characteristic dimension depends on the application, for example, in fibrous filtration it is the diameter of the fiber; in axisymmetrical impaction flows it is the radius or diameter of the impactor nozzle. For a given percent particle removal, the Stokes number value is therefore application specific. For example, the Stokes number of an impactor with one or several identical circular nozzles is

$$Stk = \frac{\rho_p d_p^2 V C_c}{9\eta d_j} \tag{4–39}$$

where $d_j$ is the impactor jet diameter in m and $V$ is the particle velocity in the jet. $V$ is assumed to be equal to the gas velocity in the jet. For further discussions of inertial devices, see Chapters 8, 9, 10, 14, and 17.

### Shape Factor

As described above, particle aerodynamic diameter and Stokes diameter have been defined using ideal spherical particles. Apart from liquid droplets or particles produced from liquid droplets, few particles in nature are spheres. It is convenient to describe more complex shapes by a single diameter and have the additional flow resistance or drag represented by a factor. This *dynamic shape factor*, $\chi$, is the ratio of the drag force of the particle in question (particle diameter, $d_p$) to that of a sphere of equivalent volume (equivalent volume diameter, $d_{ev}$). The expression for gravitational settling, Eq. 4–28, thus becomes

$$V_{grav} = \frac{\rho_p d_p^2 g C_{c,d_p}}{18\eta} = \frac{\rho_0 d_a^2 g C_{c,d_a}}{18\eta} = \frac{\rho_p d_{ev}^2 g C_{c,d_{ev}}}{18\eta\chi} \qquad Re_p < 0.1 \tag{4–40}$$

The value of the Cunningham slip factor $C_c$ depends on the chosen diameter, $d_p$, $d_a$, or $d_{ev}$. The shape factor is always equal to or greater than one. Compact shapes typically have values

between one and two, while more extreme shapes, such as fibers and high-volume agglomerates, may have larger values. Shape factors are useful for converting a readily measurable equivalent diameter to one that depends on particle behavior, such as aerodynamic diameter or diffusion equivalent diameter. Thus, shape factors have been defined in a variety of ways that have to do with the available means of measuring the physical and equivalent particle diameter as well as the means of measuring particle drag. Therefore, when applying published shape factors, it may be important to understand the experimental basis for their development.

Some particles have relatively regular shapes with volumes that can be calculated or compact shapes that can be measured with a microscope to determine an equivalent volume diameter. For such particles, the shape factor is, from Eq. 4–40,

$$\chi = \frac{\rho_p d_{ev}^2 C_{c.d_{ev}}}{\rho_0 d_a^2 C_{c.d_a}} \qquad Re_p < 0.1 \tag{4–41}$$

Three variables need to be measured: $\rho_p$, $d_{ev}$, and $d_a$. The equivalent volume diameter may be measured microscopically or determined from the mass (measured chemically or using radioactive tracers) and the number of particles (Barbe-le Borgne et al., 1986). The aerodynamic diameter can be measured in a settling chamber or centrifuge, and, if the particle contains no voids, the density is the bulk density of the particle material.

Shape factors have also been measured by settling macroscopic models of regularly shaped particles in liquids. For instance, this technique has been used to measure shape factors for cylinders and chains of spheres (Kasper et al., 1985); for rectangular prisms (Johnson et al., 1986); and for modified rectangular prisms (Sheaffer, 1987). These particles have two or three distinct symmetry axes and therefore may have two or three shape factors, depending on their orientation. Shape factors have also been derived for oblate and prolate spheroids (Fuchs, 1964:37). Table 4–3 exemplifies a few.

Porous particles, agglomerates, and fume particles may have an effective density ($r_e$, including internal voids) that is quite different from the *bulk material density*, $\rho_p$. In this case, a shape factor defined as a function of the *mass equivalent diameter* ($d_m$) may be more appro-

**TABLE 4–3. Dynamic Shape Factors for Various Types of Compact Particles (No Internal Voids)**

| Shape | Dynamic Shape Factor ($\chi$) |
|---|---|
| Sphere | 1.00 |
| Cluster of spheres | |
| 2 sphere chain | 1.12 |
| 3 sphere chain | 1.27 |
| 4 sphere chain | 1.32 |
| Prolate spheroid (L/D = 5)[a] | |
| Axis horizontal | 1.05 |
| Axis vertical | 1.39 |
| Glass Fiber(L/D = 5) | 1.71 |
| Dusts | |
| Bituminous coal | 1.05–1.11 |
| High-ash soft coal | 1.95 |
| Quartz | 1.36–1.82 |
| Sand | 1.57 |
| Talc | 2.04 |
| $UO_2$ | 1.28 |
| $ThO_2$ | 0.99 |

[a] Calculated values; all others are experimental.

*Source*: Adapted from Davies (1979).

priate (Brockmann and Rader, 1990), thus replacing $d_{ev}$ with $d_m$ in Eq. 4–41. The shape factor $\chi$ may be further broken down as the product of *envelope shape factor*, $k$, and second component $d$ (defined as $[\rho_p/\rho_e]^{1/3}$), which is due to the porosity of the particle. Theoretically or empirically derived shape factors as described above can be used to match the approximate envelopes of the observed particles. For relatively compact particles, the porosity component of $\chi$ dominates, while for more sparse, branched chain agglomerates the envelope factor dominates. For additional discussion of complex particle shapes, see Chapter 23.

## PARTICLE MOTION IN AN ELECTRIC FIELD

Application of electrostatic forces is particularly effective for submicrometer-sized particles for which gravity forces are weak because of the $d_p^3$ dependence (Eq. 4–27). On a large scale, removal of aerosols by electrostatic forces is practiced in electrostatic precipitators (also called *electrofilters*). In aerosol sampling and measuring instruments, electrostatic forces are applied to precipitate or redirect either all aerosol particles or those in a specific size range.

For a particle with a total charge equal to $n$ times the elementary unit of charge, $e$, the *electrostatic force*, $F_{elec}$, in an *electric field* of intensity, $E$, is

$$F_{elec} = neE \tag{4–42}$$

**EXAMPLE 4–5**

A 0.5 μm diameter standard density particle has been diffusion charged with 18 elementary units of charge. Calculate the electrical force on the particle when it passes between two flat parallel plates (e.g., an electrostatic precipitator) that have 5 kV applied across a 0.02 m gap. Compare the electrical to the gravitational force.

*Answer*: The electric field between the plates is

$$E = \left(\frac{5000\text{ V}}{0.02\text{ m}}\right) = 2.5\times10^5\text{ V/m}$$

$$\left[E = \left(\frac{5000\text{ V}}{2\text{ cm}}\right)\left(\frac{1\text{ stV}}{300\text{ V}}\right) = 8.33\text{ stV/cm}\right]$$

Using Eq. 4–42,

$$F_{elec} = neE = 18(1.6\times10^{-19}\text{ C})(2.5\times10^5\text{ V/m}) = 7.2\times10^{-13}\text{ N}$$

$$[F_{elec} = neE = 18(4.8\times10^{-10}\text{ stC})(8.33\text{ stV/cm}) = 7.2\times10^{-8}\text{ dyn}]$$

One newton (N) in SI units equals $10^5$ dyne in the cgs system of units. Using Eq. 3–27,

$$F_{grav} = \frac{\pi}{6}d_p^3\rho_p g = \frac{\pi}{6}(0.5\times10^{-6}\text{ m})(1000\text{ kg/m}^3)(9.80\text{ m/s}^2)$$

$$\left[F_{grav} = \frac{\pi}{6}(0.5\times10^{-4}\text{ cm})^3(1\text{ g/cm}^3)(980\text{ cm/s}^2)\right]$$

$$= 6.41\times10^{-16}\text{ N}[6.41\times10^{-11}\text{ dyn}]$$

Comparing the two forces,

$$\frac{F_{elec}}{F_{grav}} = \frac{7.2\times10^{-13}\text{ N}}{6.41\times10^{-16}\text{ N}} = 1120$$

The electric force exceeds the gravity force over 1000 times.

Electrostatic forces can affect particle motion and, to a certain extent, gas motion as well. These forces can be important during particle generation, transport, and measurement. Depending on the number of charges on a particle and the level of surrounding electric field, the force on that particle can range anywhere from zero to the largest of any force discussed here. If a particle is placed in an electric field described by Eq. 4–42, it will reach a terminal velocity, $V_{elec}$, when the field and drag forces are equal.

$$V_{elec} = \frac{neEC_c}{3\pi\eta d_p} \tag{4–43}$$

The electronic charge $e$ is $1.602 \times 10^{-19}$ coulombs (C) [$4.803 \times 10^{-10}$ statcoulombs (stC)]. This terminal or *drift velocity* can also be written in terms of the particle mobility, $B$:

$$V_{elec} = neEB \tag{4–44}$$

or, including the electric charge, the *particle electrical mobility*, $Z = neB$:

$$V_{elec} = ZE \tag{4–45}$$

where the electrical mobility, $Z$, has units of velocity/electric field or $m^2/V{\cdot}s$ [$cm^2/stV{\cdot}s$] (i.e., unit electrical mobility is a drift velocity of 1 m/s in a 1 V/m field). One statvolt (cgs unit) is equal to 300 volts (V).

**EXAMPLE 4–6**

Foundry fumes are sampled into an electrostatic precipitator for collection onto an electron microscope grid. A power supply is used to apply a potential of 5000 V across the condenser with a plate spacing, $H$, of 0.01 m. The aerosol flows through the condenser at a uniform velocity of 0.02 m/s. The particles of concern have an electrical mobility of $3.33 \times 10^{-9}$ $m^2/V{\cdot}s$. What is the minimum plate length, $L$, that will precipitate all of these particles?

*Answer*: For a potential of 5000 V, the precipitation time, $t_e$, in the electric field is

$$t_e = \frac{H}{V_{elec}} = \frac{H}{ZE} = \frac{0.01\text{m}}{\left(3.33\times10^{-9}\dfrac{\text{m}^2}{\text{V}\cdot\text{s}}\right)\left(\dfrac{5000\text{ V}}{0.01\text{ m}}\right)} = 6\text{ s}$$

In cgs units, the mobility is converted to 0.01 $cm^2/stV{\cdot}s$, and the spacing is 1 cm.

$$\left[ t_e = \frac{1\text{ cm}}{\left(0.01\dfrac{\text{cm}^2}{\text{stV}\cdot\text{s}}\right)\left(\dfrac{16.7\text{ stV}}{1\text{ cm}}\right)} = 6\text{ s} \right]$$

The transit time $t_t$ for the air flow at velocity $U$ must equal or exceed this time.

$$t_t = \frac{L}{U} \geq t_e$$

$$L \geq 6\text{ s}(0.02\text{m/s}) = 0.12\text{m}\ [12\text{ cm}]$$

The simplest electric field is uniform, for example, between two large parallel plates:

$$E = \frac{\Delta V}{x} \tag{4–46}$$

where $x$(m) is the distance between the plates and $\Delta V$ is the difference in potential (volts). The field between two concentric tubes or between a tube and a concentric wire is also

used for electrostatic precipitation. In this case the field depends on the distance, $r$, from the axis:

$$E = \frac{\Delta V}{r \ln(r_o/r_i)} \tag{4–47}$$

where $\Delta V$ is the difference in potential between the outer tube and inner tube (or wire) of radius $r_o$ and $r_i$, respectively.

In the SI units, the force in newtons (N) on each of two particles with $n_1$ and $n_2$ unit charges on them is described by *Coulomb's law*:

$$F_{elec} = \frac{n_1 n_2 e^2}{4\pi\varepsilon_0 r^2} = K_E \frac{n_1 n_2 e^2}{r^2} \tag{4–48}$$

where $r$ in m is the distance between the particles. The factor $K_E$, a proportionality constant that depends on the unit system, is $8.988 \times 10^9$ (SI units). This equation strictly applies only to point charges. However, it is a good approximation for the force between two particles or a particle at some distance from a charged object such as a sampler and indicates that the force drops off rapidly with distance. Aerosol particles, which typically carry a limited amount of charge because of their small surface area, are generally only affected electrically when they are quite close to another charged particle or close to a charged object.

In cgs units, Eq. 4–48 is converted to give the force in dynes (dyn):

$$F_{elec} = \frac{n_1 n_2 e^2}{r^2} \tag{4–49}$$

where $r$ is in cm, the electronic charge is $4.80 \times 10^{-10}$ stC, and the proportionality constant $K_E$ is unity. For further discussions of charged particle dynamics, see Chapters 17, 18, and 20.

## PARTICLE MOTION IN OTHER FORCE FIELDS

Particle motion is governed by a variety of other forces. Very small particles approach the behavior of the molecules of the surrounding gas (i.e., they diffuse readily and have little inertia); they can be affected by light pressure, acoustic pressure, and thermal pressure. In a similar fashion to gravitational and electrical forces, other forces can be used to cause particle motion and thus size-selective measurement. The same forces can also cause particles to be lost rapidly in the sampling inlet or on measurement instrument surfaces. Other forces not mentioned may have some effects but are generally much weaker than the ones mentioned here. For instance, magnetic forces are typically several orders of magnitude smaller than electrostatic forces, but have been used for fiber alignment (see Chapter 23).

### Thermophoresis

Particles in a thermal gradient are bombarded more strongly by gas molecules on the hotter side and are therefore forced away from a heat source. Thus, heated surfaces tend to remain clean, while relatively cool surfaces tend to collect particles. This process is called *thermophoresis*, from the Greek "carried by heat." For particles smaller than the mean free path ($\lambda$), the thermophoretic velocity, $V_{th}$, is independent of particle size and is (Waldmann and Schmitt, 1966)

$$V_{th} = \frac{0.55\eta}{\rho_g} \nabla T \qquad d_p < \lambda \tag{4–50}$$

where $\nabla T$ is the thermal gradient in K/m. There is a slight increase (on the order of 3%) in the velocity of rough-surfaced particles versus spherical solids or droplets.

For particles larger than $\lambda$, the thermophoretic velocity depends on the ratio of the thermal conductivity of the gas to that of the particle and also on the particle size. For large conductive aerosol particles, the thermophoretic velocity may be about five times lower than for small, nonconductive ones. To calculate the thermophoretic velocity, the molecular accommodation coefficient ($H$) is needed:

$$H \cong \left(\frac{1}{1+6\lambda/d_p}\right)\left(\frac{k_g/k_p+4.4\lambda/d_p}{1+2k_g/k_p+8.8\lambda/d_p}\right) \tag{4–51}$$

where $k_g$ and $k_p$ are the thermal conductivities of the gas and particle, respectively. The thermal conductivity of air is 0.026 W/m·K [$5.6 \times 10^{-5}$ cal/cm·s·K], while that for particles ranges from 66.9 W/m·K for a metal (iron) to 0.079 W/m·K for an insulator (asbestos) (Mercer, 1973:166). The thermally induced particle velocity is then (Waldmann and Schmidt, 1966)

$$V_{th} = \frac{-3\eta C_c H}{2\rho_g T}\nabla T \qquad d_p > \lambda \tag{4–52}$$

Thermophoresis is relatively independent of particle size over a wide range and has been used for collecting small samples, such as for electron microscope measurements, in thermal precipitators. The sampling rate of these instruments is low because of the difficulty of maintaining a thermal gradient, and thus thermal precipitators have not been scaled up for large-volume use (see Chapter 10).

### Photophoresis

Photophoresis is similar to thermophoresis in that particle motion is caused by thermal gradients at the particle surface except that in this case the heating is caused by light absorption by the particle rather than by an external source. Light shining on a particle may be preferentially absorbed by the side near the light source or, under certain circumstances of weak absorption and focusing, by the far side of the particle. Thus, in the former case the particle will be repelled from the light source, while in the latter, called *reverse photophoresis*, it will be attracted.

### Electromagnetic Radiation Pressure

Electromagnetic radiation can have a direct effect on particle motion by transferring momentum to the particle. Light impinging on a particle can be reflected, refracted, or absorbed. The fraction of momentum transfer from the light beam to the particle depends on the geometric cross section of the particle as well as the average direction of the scattered light. If a significant fraction of the light is absorbed by the particle, photophoresis, as described above, will be more important in deciding particle motion. Radiation pressure has been used to trap particles in focused laser beams and manipulate them for further study (see Chapter 20).

### Acoustic Pressure

Acoustic waves, either stationary, as in a resonant box, or traveling in open space can be reflected, diffused, or absorbed by particles. Particle motion in an acoustic field includes oscillation in response to the gas motion, circulation in the acoustic field, net drift in some direction. Such waves have been used to increase particle coagulation or agglomeration and, in other cases, to enhance droplet evaporation or condensation (Hesketh, 1977:97). A resonant acoustic system has also been used to measure particle aerodynamic diameter by measuring a particle's ability to oscillate in response to the air motion (Mazumder et al., 1979; see also Chapter 17).

### Diffusiophoresis and Stephan Flow

When the suspending gas differs in composition from one location to another, diffusion of the gas takes place. This gas diffusion results in suspended particles acquiring a net velocity as a function of the gas diffusion, that is, diffusiophoresis. The particles are pushed in the direction of the larger molecule flow. The force is a function of the molecular weight and diffusion coefficients of the diffusing gases and is largely independent of the particle size.

A special case of diffusiophoresis occurs near evaporating or condensing surfaces. A net flow of the gas–vapor mixture away from an evaporating surface is set up that creates a drag on particles. The converse situation holds for a condensing surface (i.e., gas and particles will flow toward the surface). This net motion of the gas–vapor mixture is called Stephan (also spelled Stefan) flow and can cause the motion of particles near these surfaces (Fuchs, 1964:67). Stephan flow can affect particle collection in industrial scrubbers and scavenging of the environment by growing cloud droplets. To increase particle collection by Stephan flow, the vapor must be supersaturated. Diffusiophoretic velocities are generally only significant for very small particles. For instance, diffusiophoresis of 0.005 to 0.05 μm diameter particles was found to have the following net *deposition velocity*, $V_{\text{diff}}$, toward surfaces condensing water vapor (Goldsmith and May, 1966);

$$V_{\text{diff}} = 1.9 \times 10^{-3} \frac{dP}{dx} \tag{4–53}$$

where the deposition velocity is in m/s and $dP/dx$ is the pressure gradient of the diffusing vapor in Pa/m. Note that in condensing and evaporating droplets, thermophoretic effects can also be important.

## REFERENCES


Allen, M. D. and O. G. Raabe. 1985. Slip correction measurements of spherical solid aerosol particles in an improved Millikan apparatus. *Aerosol Sci. Technol.* 4:269–286.

Barbe-le Borgne, M., D. Boulaud, G. Madelaine, and A. Renoux. 1986. Experimental determination of the dynamic shape factor of the primary sodium peroxide aerosol. *J. Aerosol Sci.* 17:79–86.

Brockmann, J. E. and D. J. Rader. 1990. APS response to nonspherical particles and experimental determination of dynamic shape factor. *Aerosol Sci. Technol.* 13:162–172.

Clift, R., J. R. Grace, and M. E. Weber. 1978. *Bubbles Drops and Particles.* New York: Academic Press.

Davies, C. N. 1979. Particle–fluid interaction. *J. Aerosol Sci.* 10:477–513.

Friedlander, S. K. 1977. *Smoke, Dust and Haze.* New York: John Wiley & Sons.

Fuchs, N. 1964. *The Mechanics of Aerosols.* Oxford: Pergamon Press. (Reprinted Mineola, NY: Dover Press, 1989.)

Goldsmith, P. and F. G. May. 1966. In *Aerosol Science*, ed. C. N. Davies. London: Academic Press.

Hesketh, H. E. 1977. *Fine Particles in Viscous Media.* Ann Arbor, MI: Ann Arbor Science Publishers.

Hinds, W. C. 1999. *Aerosol Technology.* New York: John Wiley & Sons.

Johnson, D. L., D. Leith, and P. C. Reist. 1987. Drag on non-spherical, orthotropic aerosol particles. *J. Aerosol Sci.* 18:87–97.

Kasper, G., T. Niida, and M. Yang. 1985. Measurements of viscous drag on cylinders and chains of spheres with aspect ratios between 2 and 50. *J. Aerosol Sci.* 16:535–556.

Licht, W. 1988. *Air Pollution Control Engineering: Basic Calculations for Particulate Collection.* New York: Marcel Dekker, Inc.

Mazumder, M. K., R. E. Ware, J. D. Wilson, R. G. Renninger, F. C. Hiller, P. C. McLeod, R. W. Raible, and M. K. Testerman. 1979. SPART analyzer: Its application to aerodynamic size measurement. *J. Aerosol Sci.* 10:561–569.

McConalogue, D. J. and R. S. Srivastava. 1968. Motion of a fluid in a curved tube. *Proc. R. Soc. A.* 307:37–53.

Mercer, T. T. 1973. *Aerosol Technology in Hazard Evaluation.* New York: Academic Press.

Rader, D. J. 1990. Momentum slip correction factor for small particles in nine common gases. *J. Aerosol Sci.* 21:161–168.

Sartor, J. D. and C. E. Abbott. 1975. Prediction and measurement of the accelerated motion of water drops in air. *J. Appl. Meteorol.* 14(2):232–239.

Schlichting, H. 1979. *Boundary-Layer Theory.* New York: McGraw Hill.

Sheaffer, A. W. 1987. Drag on modified rectangular prisms. *J. Aerosol Sci.* 18:11–16.

Tsai, C. J. and D. Y. H. Pui. 1990. Numerical study of particle deposition in bends of a circular cross-section–laminar flow regime. *Aerosol Sci. Technol.* 12:813–831.

Waldmann, L. and K. H. Schmitt. 1966. Thermophoresis and diffusiophoresis of aerosols. In *Aerosol Science*, ed. C. N. Davies. London: Academic Press.

White, F. M. 1986. *Fluid Mechanics.* New York: McGraw-Hill.

Willeke, K. 1976. Temperature dependence of particle slip in a gaseous medium. *J. Aerosol Sci.* 7:381–387.

# AEROSOL MEASUREMENT

## Principles, Techniques, and Applications

**SECOND EDITION**

*Edited by*

**Paul A. Baron, Ph.D.**
*Physical Scientist*
*Centers for Disease Control and Prevention*
*National Institute for Occupational Safety and Health*
*Cincinnati, OH*

**Klaus Willeke, Ph.D.**
*Professor*
*Department of Environmental Health*
*University of Cincinnati*
*Cincinnati, OH*

WILEY-INTERSCIENCE

A JOHN WILEY & SONS, INC., PUBLICATION

New York • Chichester • Weinheim • Brisbane • Singapore • Toronto

This book is printed on acid-free paper. ♾



Published simultaneously in Canada.



***Library of Congress Cataloging-in-Publication Data:***

Aerosol measurement : principles, techniques, and applications / [edited] by Paul A. Baron and Klaus Willeke.—2nd ed.

p. cm.

Includes index.

ISBN 0-471-35636-0 (cloth)

1. Aerosols—Measurement. 2. Air—Pollution—Measurement. I. Baron, Paul A., 1944– II. Willeke, Klaus.

TD884.5 .A33 2001

628.5'3'0287–dc21 2001017845

Printed in the United States of America.

10 9 8 7 6 5 4 3 2 1